NUMERICAL INVESTIGATION OF MIXED FLOWS TURBOFAN ENGINE THRUST CORRELATED WITH THE COMBUSTION CHAMBER'S PARAMETERS

Irina-Carmen ANDREI[*], Constantin ROTARU[**], Maria-Cristina FADGYAS[*], Gabriela STROE[***], Mihai Leonida NICULESCU[*],

[*]National Institute for Aerospace Research "Elie Carafoli" (andrei.irina@incas.ro, niculescu.mihai@incas.ro)
[**]"Henri Coanda" Air Force Academy, Brasov, Romania (rotaru.constantin@yahoo.com)
[***]"POLITEHNICA" University of Bucharest, Faculty of Aerospace Engineering, (ing.Stroe@yaoo.com)

DOI: 10.19062/2247-3173.2017.19.1.3

Abstract: *The purpose of this paper is to show the influence of the most relevant parameters of the combustion chamber (e.g. perturbations in the turbine inlet temperature T3T and pressure losses) and the predicted performances of a mixed flows turbofan engine. The performances of the mixed flow turbofan engine have been predicted by following the numerical simulation of the engine's operation, with an in-house developed code, based on a comprehensive mathematical model of the mixed flow turbofan engine. The investigation is carried on at the engine's design point, which means 100% rotational speed, at sea level static standard atmosphere conditions. The most significant parameters of the combustion chamber, namely the combustion chamber's pressure losses and the perturbations in the turbine inlet temperature T3T have been chosen such that to match the standpoint of the fighter pilot; the most relevant parameter is the turbine inlet temperature T3T. The numerical results are summarized as graphs and charts, from which one can express new correlations and further, a new command and control law for the turbojet engine's operation can be concluded. The contributions of this study may prove to have practical applications, for being used both for training the pilot students and during flight operation, for contributing to a significant improvement in flight safety, which can be of real help for fighter pilots.*

Keywords: *mixed flows turbofan engine, performance prediction, combustion chamber, numerical simulation, engine maps*

1. INTRODUCTION

There are certain advantages provided by the use of the turbofan engines; the most important feature is that for twin- or triple-spool constructions, the engine operates much far from the surge line, for the entire flight envelope. The constructive differences between turbojet and turbofan engine can be noticed from the schematic diagram, Fig. 1.

Large by pass turbofans are shown in Fig. 1 - c, d, which are also referred as just turbofan; the object of this study is the mixed flows turbofan, presented in Fig. 1-a.

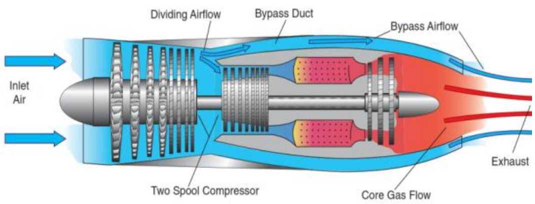

(a) Mixed Flows Turbofan

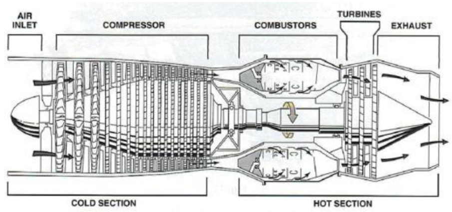

(b) Turbojet

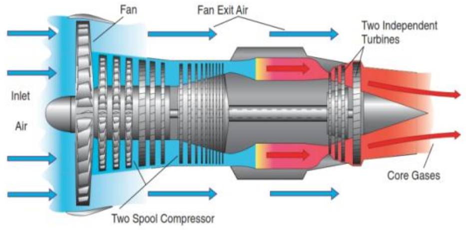

(c) Twin spool Turbofan

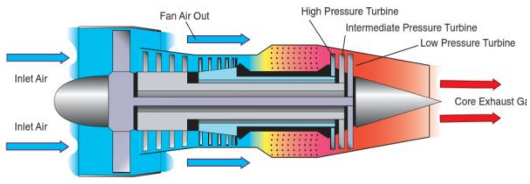

(d) Triple spool Turbofan

FIG. 1 - Schematic diagrams, [2-3]

The parameters of the combustion chamber, from the standpoint of the jet engine performances, are the turbine inlet temperature T3T [K], the pressure loss coefficient, compressor exit temperature and the properties of the fuel, which for most of the cases are represented by the fuel specific power P_{ci}; taking into account the following assumptions: 1/ that the combustion chamber is designed such that the pressure losses should be minimized, and therefore the pressure loss coefficient remains quasi constant, its magnitude being around 0.98, 2/ that the fuel specific power is with two orders of magnitude higher than the largest value of the stagnation specific enthalpy at turbine inlet, no matter that the fuel specific power is ranging from 40000 up to 45000 [kJ/kg], 3/ the variation of the compressor exit temperature is not so large and does not influence the turbojet performances, because the variation of the compressor pressure ratio (as shown by the compressor universal map) is limited; therefore, the investigation presented in this paper can be focused on the influence of the variation of the turbine inlet temperature, altitude and Mach number as flight parameters and speed as engine operating regime.

The **study case** is a mixed flows turbofan, as detailed in Fig. 1-a, defined by the main engine parameters: overall pressure ratio π_c^* = 22, by pass ratio ***K*** = 2.9, overall airflow rate $\dot{M}_a$ = 65.772 [kg/s]; following the identification of missing design parameters, there have been determined, Andrei I. [15, 18], the Turbine inlet temperature T3T = 1410 [K], then the fan pressure ratio π_v^* = 1.76, which corresponds to the optimum fan specific work l_v^* = **59.657** [kJ/kg]; eventually, at SLS level, ISA is calculated the maximum Thrust F = 20.91 [kN] (military thrust).

Other parameters required for calculating the performances of the engine are: air intake pressure loss, adiabatic efficiency on compression for compressor and for the fan, combustion chamber pressure loss, adiabatic efficiency on turbine expansion, velocity loss within nozzle exit, mechanical efficiency (i.e. shaft transmission efficiency). The specificity of the mixed flows turbofan is the mixing of the two streams, meaning the primary stream of burned gas and the secondary stream of compressed air; therefore, the parameters at fan exit and turbine exit are important for calculating the overall engine thrust; the parameters in question are: turbine exit stagnation pressure p_4^* and stagnation temperature T_4^*, fan air exit stagnation pressure p_{2v}^* and stagnation temperature T_{2v}^* and combustor fuel – air mixture ratio α .

The **objectives** of the analysis of the mixed flows turbofan MFTF engine are represented by modeling and simulation, in purpose to obtain the predicted engine performances, for different flight regimes and various operating regimes. Basically, the construction of a MFTF ENGINE Model supposes the completion of the steady state analysis, which supposes the calculation of the Brayton cycle at Sea Level Static SLS and ISA conditions, followed by the calculation of turbojet performances (thrust, specific thrust and fuel specific consumption, such that to build the engine's Operation Maps, which are: 1/ the Altitude Map, 2/ the Velocity Map, 3/ the Rotor Speed Map and 4/ the engine's Universal Map.

2. PERFORMANCE ANALYSIS OF MIXED FLOWS TURBOFAN ENGINE

2.1 Problem statement and framework

Performance Analysis of Mixed Flows Turbofan Engine, supposes the completion of three phases; thorough details are given in literature, Mattingly [1], as well as authors other researches, Andrei [8-15, 17-18], Rotaru [21-23] and Prisacariu [16].

The first phase consists in calculating at SLS, ISA conditions (i.e. "*fixed point*", which usually means altitude H = 0 [km] and flight velocity V = 0 [m/s]) of the engine's performances (*Thrust*, *Specific Thrust*, *Specific Fuel Consumption*) and the determination of the engine's thermodynamic cycle (i.e. Brayton cycle).

The second phase consists in calculating the engine's performances at different flight regimes and rotor speed, which usually are expressed by **ENGINE's OPERATING MAPS** (i.e. **ALTITUDE MAP, VELOCITY MAP, SPEED MAP**.

The third phase, which consists in calculating of the **ENGINE's UNIVERSAL MAP**, completes the performance analysis. The results obtained following the performance analysis of the engine allow to study the dynamic behaviour of the engine and to do the numerical simulations.

2.2 Mathematical support

The performances of the mixed flows turbofan can be calculated from relations (1) ÷ (9) presented below; the thrust of a mixed flows turbofan is expressed by the variation (1) of flow and velocity between the inlet and exit sections of the engine; the specific thrust is defined by relation (2), while the definition of specific fuel consumption is one of the equations (5-7,9). The order at calculating the performances of the mixed flows turbofan is that first is determined the specific thrust F_{sp} [Ns/kg], then the thrust F [N] and fuel specific consumption C_{sp} [kg/Nh]. The relations expressing the performances of the mixed flows turbofan engine are valid for all flight regimes and engine running conditions.

$$F = \dot{M}_{am} \cdot C_{5am} - \dot{M}_a \cdot V \tag{1}$$

$$F_{sp} = \frac{F}{\dot{M}_{a1}} \tag{2}$$

$$F = \dot{M}_{am} \cdot (1+K) \cdot C_{5am} - \dot{M}_a \cdot (1+K) \cdot V \tag{3}$$

$$F = \dot{M}_{am} \cdot (1+K) \cdot (C_{5am} - V) \tag{4}$$

$$C_{sp} = 3600 \cdot \frac{\dot{M}_c}{F} \tag{5}$$

$$C_{sp} = 3600 \cdot \frac{\dot{M}_c}{\dot{M}_{a1}} \cdot \frac{1}{F_{sp}} \tag{6}$$

$$C_{sp} = 3600 \cdot \frac{m_c}{F_{sp}} \tag{7}$$

$$F_{sp} = (1+K) \cdot (C_{5am} - V) \tag{8}$$

$$C_{sp} = 3600 \cdot \frac{m_c}{(1+K) \cdot (C_{5am} - V)} \tag{9}$$

The airflow at mixing area $\dot{M}_{4am}$ area results from the mainstream gas flow $\dot{M}_g$ and the secondary stream airflow $\dot{M}_{a2}$; taking into account that the gas flow results as a mixture of air and hot gas and after having neglected the fuel flow with respect to the airflow, then the airflow at mixing area becomes proportional with the bypass ratio and the mainstream airflow.

$$\dot{M}_c << \dot{M}_{a1} \tag{10}$$

$$\dot{M}_g = \dot{M}_{a1} + \dot{M}_c \tag{11}$$

$$\dot{M}_g \approx \dot{M}_{a1} \tag{12}$$

$$\dot{M}_{4am} = \dot{M}_g + \dot{M}_{a2} \tag{13}$$

$$\dot{M}_{4am} \approx \dot{M}_{a1} + \dot{M}_{a2} \tag{14}$$

$$\dot{M}_{4am} \approx \dot{M}_{a1} \cdot (1+K) \tag{15}$$

For the particular case of the engine running at SLS, ISA conditions, which in literature is also referred as the "*design point*" or the “*fixed point regime*”, the performances of the MFTF engine at fixed point conditions (SLS, ISA) are given by the simplified relations (16-18).

$$F_{sp0} = (1+K_0) \cdot C_{5am\_0} \quad (16) \qquad F_0 = F_{sp0} \cdot \dot{M}_{a10} \quad (17) \qquad C_{sp0} = 3600 \cdot \frac{m_{c0}}{F_{sp0}} \quad (18)$$

The expressions connecting the **air flowrates on main and secondary streams** are as follows: being given the airflow of both streams $\dot{M}_a$ = 65.772 [kg/s] and the by-pass ratio, then the airflow of mainstream $\dot{M}_{a1}$ and the airflow on secondary stream $\dot{M}_{a2}$ are deduced as the solutions of a linear system of equations; the index "0" refers to the parameters values at fixed point condition.

$$K = \frac{\dot{M}_{a2}}{\dot{M}_{a1}} \tag{19}$$

$$\dot{M}_a = \dot{M}_{a1} + \dot{M}_{a2} \tag{20}$$

$$\dot{M}_{a1} = \frac{\dot{M}_a}{(1+K)} \tag{21}$$

$$\dot{M}_{a10} = 16.865 \text{ [kg/s]} \tag{21.0}$$

$$\dot{M}_{a2} = \frac{K}{(1+K)} \cdot \dot{M}_a \tag{22}$$

$$\dot{M}_{a20} = 48.907 \text{ [kg/s]} \tag{22.0}$$

The influence of the altitude, Mach number and speed variation has effects not just on the performances of the mixed flows turbofan engine, but on the specific work of the compressor and fan, on compressor pressure ratio and fan pressure ratio, on the fluid flow rates on both streams, on by-pass ratio and dynamic pressure ratio. An excerpt of the calculations are exposed in the following:

The variation of the specific work of compressor and fan with the flight regimes is expressed by the corresponding values at fixed point and the square of the ratio of the speeds $\overline{n}$ at off-design versus design regimes. For computing the altitude map and velocity map and/ or the universal map of the engine, the ratio of the speeds $\overline{n}$ is equal to the unity, meaning that the engine is running at the design regime speed.

$$\overline{n} = \frac{n_{off-design}[rpm]}{n_{design}[rpm]} \tag{23}$$

$$l_c^* = l_{c0}^* \cdot \overline{n}^2 \tag{24}$$

$$l_v^* = l_{v0}^* \cdot \overline{n}^2 \tag{25}$$

The relations between the **specific work** of compressor l_c^* [kJ/kg] and fan l_v^* [kJ/kg] and pressure ratio and specific stagnation enthalpy at air intake i_1^* [kJ/kg] are (25) and (26); for the fixed point regime, the relations (25.0) and (26.0) are likewise, but with different proportion factor, which is the specific enthalpy $i_0 \approx 288$ [kJ/kg].

$$l_c^* = i_1^* \cdot \frac{\left(\left(\pi_c^*\right)^{\left(\frac{k}{k-1}\right)} - 1 \right)}{\eta_c^*} \tag{25}$$

$$l_v^* = i_1^* \cdot \frac{\left(\left(\pi_v^*\right)^{\left(\frac{k}{k-1}\right)} - 1 \right)}{\eta_v^*} \tag{26}$$

From equation $\eta_m \cdot l_t^* = l_c^* + K \cdot l_v^*$ (27) which expresses the engine's work balance, the turbine specific work l_t^* [kJ/kg] is calculated. Therefore, at fixed point regime, the work balance shows l_{c0}^* = 477 [kJ/kg], l_{v0}^* = 57.6 [kJ/kg] and l_{t0}^* = 645.3 [kJ/kg].

$$l_{c0}^* = i_0 \cdot \frac{\left(\left(\pi_{c0}^*\right)^{\left(\frac{k}{k-1}\right)} - 1 \right)}{\eta_{c0}^*} \tag{25.0}$$

$$l_{v0}^* = i_0 \cdot \frac{\left(\left(\pi_{v0}^*\right)^{\left(\frac{k}{k-1}\right)} - 1 \right)}{\eta_{v0}^*} \tag{26.0}$$

The variation of the compressor pressure ratio (27) and fan pressure ratio (28) with the flying regime and engine speed.

$$\pi_c^* = \left(1 + \overline{n}^2 \cdot \left(\frac{i_0}{i_1^*} \right) \cdot \left(\frac{\eta_c}{\eta_{c0}} \right) \cdot \left[\left(\pi_{c0}^* \right)^{\left(\frac{k-1}{k}\right)} - 1 \right] \right)^{\left(\frac{k}{k-1}\right)} \tag{27}$$

$$\pi_v^* = \left(1 + \overline{n}^2 \cdot \left(\frac{i_0}{i_1^*} \right) \cdot \left(\frac{\eta_v}{\eta_{v0}} \right) \cdot \left[\left(\pi_{v0}^* \right)^{\left(\frac{k-1}{k}\right)} - 1 \right] \right)^{\left(\frac{k}{k-1}\right)} \tag{28}$$

The **dynamic pressure ratio** is defined (29) as the ratio of the stagnation versus static pressure at known altitude H [km]. After introducing the thermodynamic function $\theta(M)$ of argument being the Mach number, then other equations are deduced for the dynamic pressure ratio π_d^*.

$$\pi_d^* = \left(\frac{p_H^*}{p_H}\right) \tag{29}$$

$$\theta(M) = \left(\frac{T_H^*}{T_H}\right) \tag{30}$$

$$\theta(\lambda) = \left(\frac{T_H}{T_H^*}\right) \tag{31}$$

$$\theta(M) = \left(1 + \frac{k-1}{2} \cdot M^2\right) \tag{32}$$

$$\theta(\lambda) = \left(1 - \frac{k-1}{k+1} \cdot \lambda^2\right) \tag{33}$$

$$\left(\frac{p_H^*}{p_H}\right) = \left(\frac{T_H^*}{T_H}\right)^{\left(\frac{k}{k-1}\right)} \tag{34}$$

$$\pi_d^* = \left(\frac{T_H^*}{T_H}\right)^{\left(\frac{k}{k-1}\right)} \tag{35}$$

$$\pi_d^* = \left[\theta(M)\right]^{\left(\frac{k}{k-1}\right)} \tag{36}$$

$$\pi_d^* = \left[\theta(\lambda)\right]^{-\left(\frac{k}{k-1}\right)} \tag{37}$$

The variation of the **bypass ratio** (38):

$$K = K_0 \cdot \left(\frac{\pi_v^*}{\pi_{v0}^*}\right)\left(\frac{\pi_{c0}^*}{\pi_c^*}\right) \cdot q\left(\bar{\lambda}_{52}\right) \cdot \sqrt{\frac{\left(i_0 + l_{v0}^*\right)}{\left(i_1^* + l_{v0}^*\right)}} \tag{38}$$

This equation correlates the variation of the bypass ratio with the pressure ratios of fan and compressor, specific work of fan at fixed point l_{v0}^*, velocity coefficient λ and enthalpy at intake i_0 and i_1^* for fixed point and flight conditions respectively. With the thermodynamic flow function $q(\lambda)$, the dimensionless parameter $q\left(\bar{\lambda}_{52}\right)$ is obtained.

$$q\left(\bar{\lambda}_{52}\right) = \frac{q\left(\lambda_{52}\right)}{q\left(\lambda_{52\_0}\right)} \tag{39}$$

$$q(\lambda) = \lambda \cdot \left[\frac{k+1}{2} \cdot \left(1 - \left(\frac{k-1}{k+1}\right) \cdot \lambda^2\right)\right]^{\frac{1}{k-1}} \tag{40}$$

$$\theta(\lambda) = \left(1 - \frac{k-1}{k+1} \cdot \lambda^2\right) \tag{41}$$

$$a_{cr} = \sqrt{2 \cdot \frac{k}{k+1} \cdot R \cdot T^*} \quad (42)$$

$$i_1^* = i_H^* = i_H + \frac{V^2}{2} \quad (43)$$

$$i_H^* = i_H \cdot \left[\theta(M) \right] \quad (44)$$

The variation of **air flow on mainstream** is given by relation (45) and of airflow on secondary stream is then $\dot{M}_{a2} = K \cdot \dot{M}_{a1}$ (46), allowing to determine the airflow on both streams $\dot{M}_a = \dot{M}_{a1} + \dot{M}_{a2}$ (47); the variation of the both airflows with the flight regimes is influenced by the variation of the pressure ratio and bypass ratio with the flight regimes, the work done by the fan and inlet enthalpy for SLS, ISA and flight altitude, ISA.

$$\dot{M}_{a1} = \dot{M}_{a10} \cdot \frac{\pi_c^*}{\pi_{c0}^*} \cdot \pi_d^* \cdot \frac{p_H}{p_0} \quad (45)$$

The exhaust velocity of the mixed streams allows the calculation of specific thrust and thrust; it is defined by the drop of stagnation enthalpy between the mixing zone and engine' exhaust; the equivalent relation expresses the link between the exhaust velocity with the stagnation enthalpy in the mixing area and the ratio of stagnation pressures.

$$C_{5am} = \varphi_{ar\_am} \cdot \sqrt{2 \cdot \left(i_{4am}^* - i_{5am\_id} \right)} \quad (48)$$

$$C_{5am} = \varphi_{ar\_am} \cdot \sqrt{2 \cdot i_{4am}^* \cdot \left(1 - \left(\frac{p_5}{p_{4am}^*} \right)^{\left(\frac{k_g - 1}{k_g} \right)} \right)} \quad (49)$$

$$C_{5am} = \varphi_{ar\_am} \cdot \sqrt{2 \cdot i_{4am}^* \cdot \left(1 - \left(\frac{p_H}{p_{4am}^*} \right)^{\left(\frac{k_g - 1}{k_g} \right)} \right)} \quad (50)$$

Usually, the exhaust velocity is calculated with the relation (49), which is valid for fully expansion, or with its equivalent (50) for partial expansion.

$$C_{5am} = \varphi_{ar\_am} \cdot \sqrt{2 \cdot i_{4am}^* \cdot \left(1 - (0.543)^{\left(\frac{k_g - 1}{k_g} \right)} \right)} \quad (51)$$

Fully expansion of core exhaust gases (down to ambient pressure) allows the obtaining of the maximum thrust, and occurs at take off; for the flight regimes, the core exhaust gases are partially expanded, down to the critical pressure.

$$p_{cr} \approx 0.543 \cdot p_{4am}^* \quad (52)$$

$$\begin{cases} if \left(p_{cr} \le p_H \right) \\ then \left(p_5 = p_H \right) \end{cases} \quad (53)$$

$$\begin{cases} if \left(p_{cr} > p_H \right) \\ then \left(p_5 = p_{cr} \right) \end{cases} \quad (54)$$

The critical pressure aft turbine p_{cr} is an important parameter for determining the conditions for fully expansion (53) of partially expansion (54) of the mixing stream at exhaust. According to the nature of the expansion (i.e. fully versus partially), the exhaust velocity C_{5am} and then the performances of the engine (i.e. the specific thrust F_{sp}, thrust F and specific fuel consumption C_{sp}) can be calculated.

The critical pressure aft turbine p_{cr} (52) is calculated after the determination of the stagnation pressure at mixing area p^*_{4am} from the relation (55).

$$(1+K)\cdot\frac{\sqrt{T^*_{4am}}}{p^*_{4am}}\cdot\frac{1}{q(\lambda_{4am})}=\frac{\sqrt{T^*_4}}{p^*_4}\cdot\frac{1}{q(\lambda_4)}+K\cdot\frac{\sqrt{T^*_{2v}}}{p^*_{2v}}\cdot\frac{1}{q(\lambda_{2v})} \tag{55}$$

The calculation of the incoming and outgoing parameters from the mixing area is based on the mixing area model; from the condition that the velocities and pressures (static or stagnation) must be equal, is deduced, Andrei I. [15], a non linear equation (56) or (57) for the identification of the turbine inlet temperature T3T, which can be solved numerically.

$$\pi^*_c\cdot\sigma^*_{ca}\cdot\left(1-\left(\frac{l^*_c+K\cdot l^*_v}{\eta^*_t\cdot i^*_3}\right)\right)^{\left(\frac{k_g}{k_g-1}\right)}=\left(1+\left(\frac{l^*_v\cdot\eta^*_v}{i^*_1}\right)\right)^{\left(\frac{k}{k-1}\right)} \tag{56}$$

$$\ln\left(\pi^*_c\cdot\sigma^*_{ca}\right)+\left(\frac{k_g}{k_g-1}\right)\cdot\ln\left(1-\left(\frac{l^*_c+K\cdot l^*_v}{\eta^*_t\cdot i^*_3}\right)\right)=\left(\frac{k}{k-1}\right)\cdot\ln\left(1+\left(\frac{l^*_v\cdot\eta^*_v}{i^*_1}\right)\right) \tag{57}$$

Based on the conservation laws for mass, momentum and energy (58-60), the governing equations for the mixing area (61-62) are deduced:

Mass conservation $$\dot{M}_{4am}=\dot{M}_{a1}\cdot(1+K) \tag{58}$$

Momentum conservation $$(1+K)\cdot\sqrt{T^*_{4am}}\cdot z(\lambda_{4am})=\sqrt{T^*_4}\cdot z(\lambda_{4g})+K\cdot\sqrt{T^*_{2v}}\cdot z(\lambda_{2v}) \tag{59}$$

Energy conservation $$(1+K)\cdot i^*_{4am}=i^*_4+(1+K)\cdot i^*_{2v} \tag{60}$$

$$(1+K)\cdot\frac{\sqrt{T^*_{4am}}}{p^*_{4am}}\cdot\frac{1}{q(\lambda_{4am})}=\frac{\sqrt{T^*_4}}{p^*_4}\cdot\frac{1}{q(\lambda_4)}+K\cdot\frac{\sqrt{T^*_{2v}}}{p^*_{2v}}\cdot\frac{1}{q(\lambda_{2v})} \tag{61}$$

$$\lambda_4\cdot(1+K)+\frac{1}{\lambda_4}\cdot\left(1+K\cdot\frac{T^*_{2v}}{T^*_4}\right)=(1+K)\cdot\sqrt{\frac{T^*_{4am}}{T^*_4}}\cdot\left(\lambda_{4am}+\frac{1}{\lambda_{am}}\right) \tag{62}$$

The solutions are the roots (64) of the second order parabola (63); taking into account that the velocity coefficient (65) is always less than the unity, then there is only one valid value for the solution.

$$(\lambda_4)^2\cdot(1+K)-(\lambda_4)\cdot(1+K)\cdot\sqrt{\frac{T^*_{4am}}{T^*_4}}+\left(1+K\cdot\frac{T^*_{2v}}{T^*_4}\right)=0 \tag{63}$$

$$(\lambda_4)_{1,2}=\frac{1}{2}\cdot\left(\sqrt{\frac{T^*_{4am}}{T^*_4}}\pm\sqrt{\frac{T^*_{4am}}{T^*_4}-\frac{4}{(1+K)}\cdot\left(1+K\cdot\frac{T^*_{2v}}{T^*_4}\right)}\right) \tag{64}$$

$$\lambda\in[0,1]\subseteq\Re \tag{65}$$

$$\lambda_{2v} = \lambda_4 \cdot \sqrt{\frac{T_4^*}{T_{2v}^*}} \qquad (66)$$

Therefore, the velocity coefficients for the main stream λ_4 (60) and secondary stream λ_{2v} (49) are determined analytically, both ranging the interval [0,1].

The mathematical model of a jet engine is completed by the assumptions regarding the properties of the fluids: 1/ the working fluid is considered perfect gas, 2/ two species:

A. // **air** // - from intake to compressor,

B. // **burned gas** // - within combustor, turbine and exhaust unit,

3/ fuel specific power, for JET A, JET A1 and/or JET B (aviation kerosene): $P_{CI} = 43500 \left[\frac{kJ}{kg}\right]$, 4/ ratio of specific heat $k = \frac{C_p}{C_v}$, see Table 1; 5/ constant pressure specific heat C_p $[\frac{kJ}{kgK}]$; 6/ gas constant R $\left[\frac{kJ}{kgK}\right]$; the relation between R and C_p is (67):

$$C_p = R \cdot \frac{k}{k-1} \qquad (67)$$

Table 1 - Properties of the working fluids

Fluid	k	C_p [kJ/kg/K]	R [J/kg/K]
Air	1.4	1.005	287.3
Burned Gas	1.33	1.165	288.4

The mathematical model of a mixed flows turbofan includes the mathematical model of a turbojet engine, since the latter describes the mainstream fluid flow thermo-dynamical processes.

The results from the simulation the Mixed Flows Turbofan Engine are summarized and presented graphically as the engine operating maps (i.e. the altitude map, the velocity map, the rotor speed map) and the engine's universal map; their definitions are introduced in the following, taking into account that these maps express the variation of the jet engine performances: thrust F [N], specific thrust F_{sp} [Ns/kg] and specific fuel consumption C_{sp} [kg/Nh] or TSFC, with altitude, flight velocity and engine rotational regime)

4. RESULTS

This investigation is focused on highlighting the influence of the turbine inlet temperature, as the most significant parameters of the combustion chamber, upon the turbojet engine's performances. With respect to the engine's design point parameters, i.e. the turbine inlet temperature being 1410 [K], it was considered a ranging interval from 1360 [K] up to 1460 [K], which corresponds to a perturbation of temperature with 50 [K], up and down with respect to the reference value.

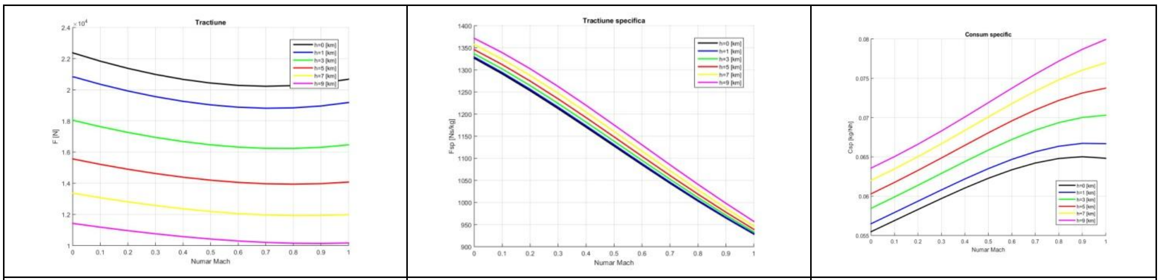

a)- Thrust [N] | b)- Specific Thrust [Ns/kg] | c)- Fuel Specific Cons. [kg/Nh]

FIG. 1 - Engine Performances from Altitude Map, T3T =1410 [K], design speed =1

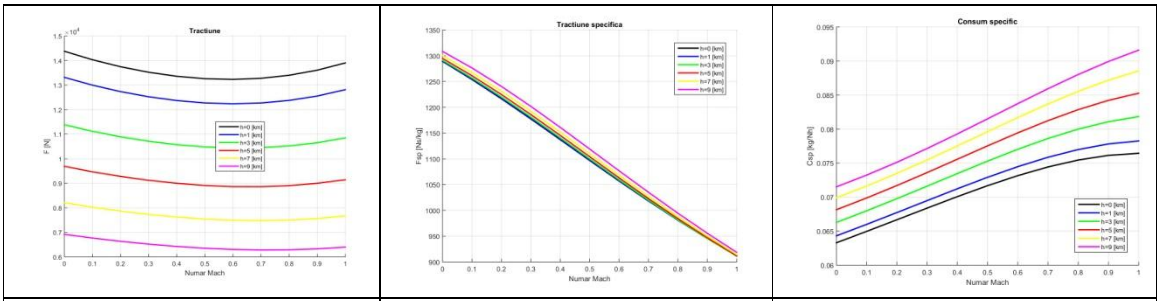

a)- Thrust [N] | b)- Specific Thrust [Ns/kg] | c)- Fuel Specific Cons. [kg/Nh]

FIG. 2 - Engine Performances from Altitude Map, T3T =1410 [K], cruise speed =0.9

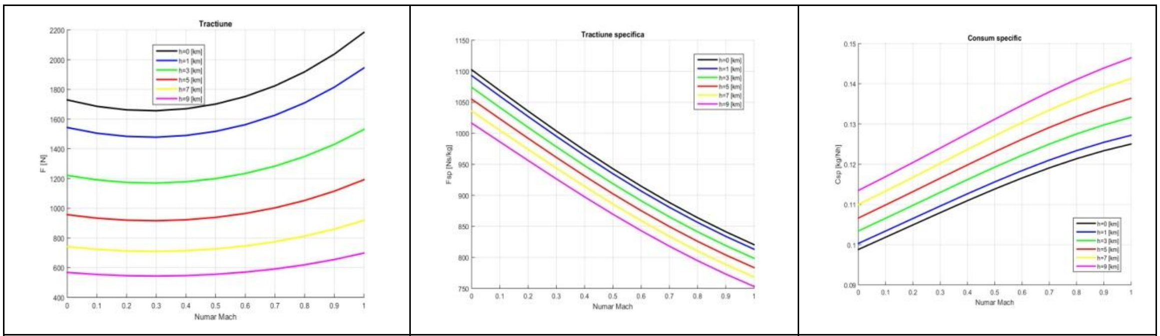

a)- Thrust [N] | b)- Specific Thrust [Ns/kg] | c)- Fuel Specific Cons. [kg/Nh]

FIG. 3 - Engine Performances from Altitude Map, T3T =1410 [K], ground idling speed =0.4

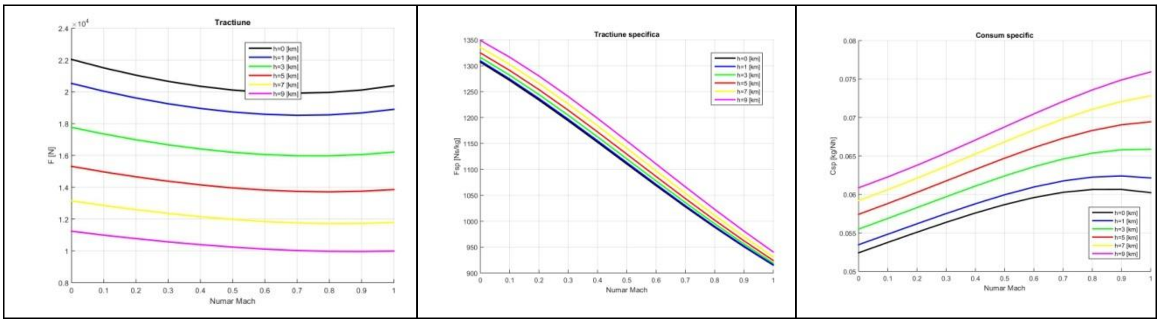

a)- Thrust [N] | b)- Specific Thrust [Ns/kg] | c)- Fuel Specific Cons. [kg/Nh]

FIG. 4 - Engine Performances from Altitude Map, T3T =1360 [K], design speed =1

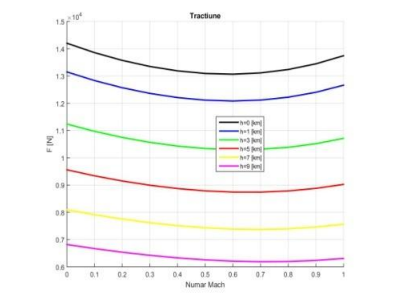

a)- Thrust [N]

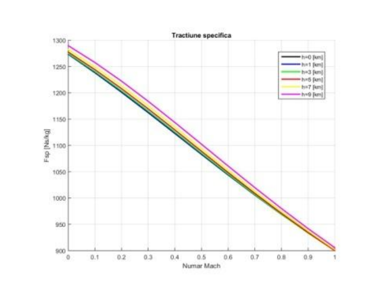

b)- Specific Thrust [Ns/kg]

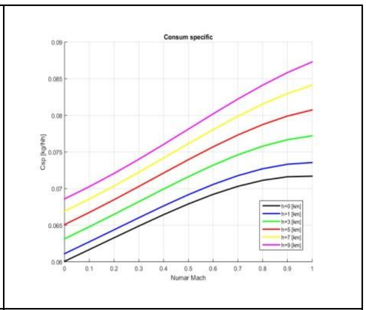

c)- Fuel Specific Cons. [kg/Nh]

FIG. 5 - Engine Performances from Altitude Map, T3T =1360 [K], cruise speed =0.9

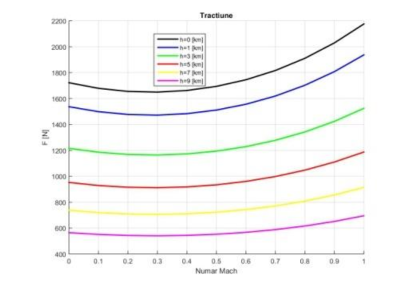

a)- Thrust [N]

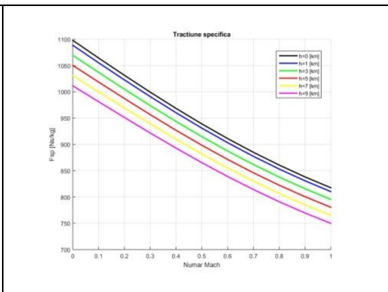

b)- Specific Thrust [Ns/kg]

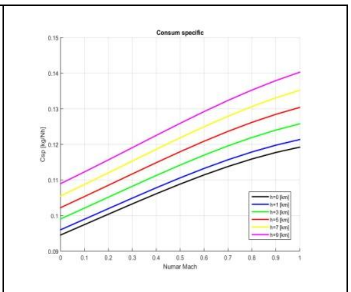

c)- Fuel Specific Cons. [kg/Nh]

FIG. 6 - Engine Performances from Altitude Map, T3T =1360 [K], ground idling speed =0.4

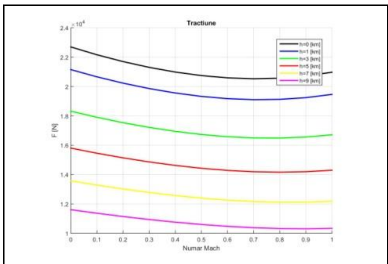

a)- Thrust [N]

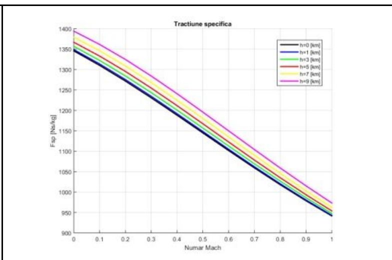

b)- Specific Thrust [Ns/kg]

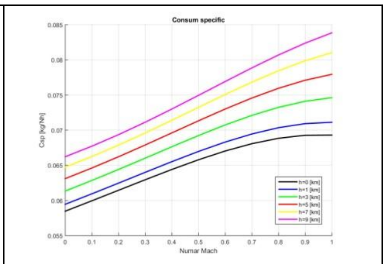

c)- Fuel Specific Cons. [kg/Nh]

FIG. 7 - Engine Performances from Altitude Map, T3T =1460 [K], design speed =1

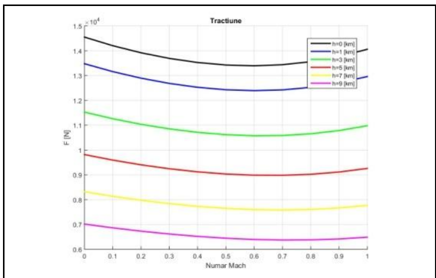

a)- Thrust [N]

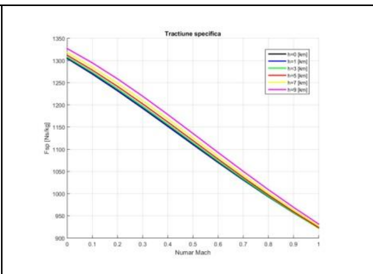

b)- Specific Thrust [Ns/kg]

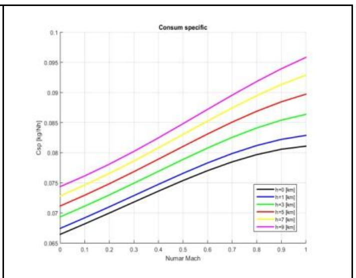

c)- Fuel Specific Cons. [kg/Nh]

FIG. 8 - Engine Performances from Altitude Map, T3T =1460 [K], cruise speed =0.9

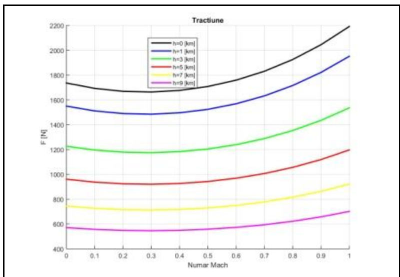

a)- Thrust [N]

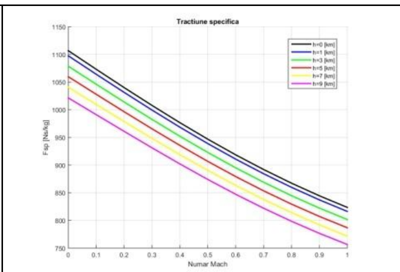

b)- Specific Thrust [Ns/kg]

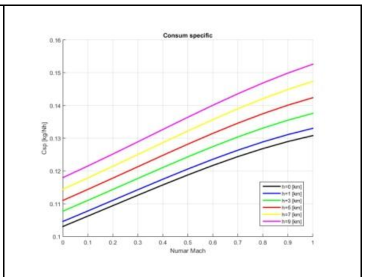

c)- Fuel Specific Cons. [kg/Nh]

FIG. 9 - Engine Performances from Altitude Map, T3T =1460 [K], ground idling speed =0.4

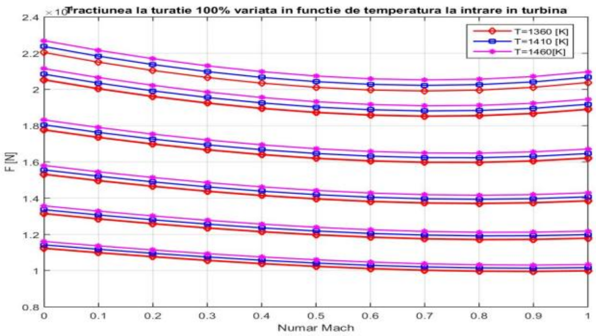

FIG. 10 - Comparison of Engine Thrust [N]. design speed = 1, T3T =1360, 1410, 1460 [K],

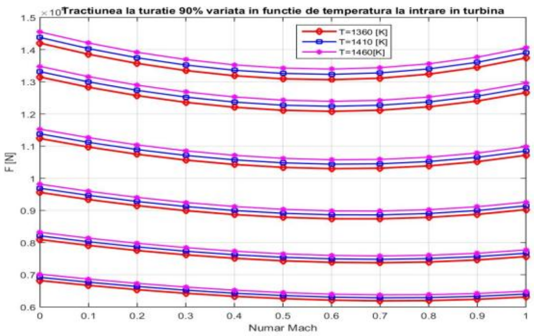

FIG. 11 - Comparison of Engine Thrust [N]. cruise speed = 0.9, T3T =1360, 1410, 1460 [K],

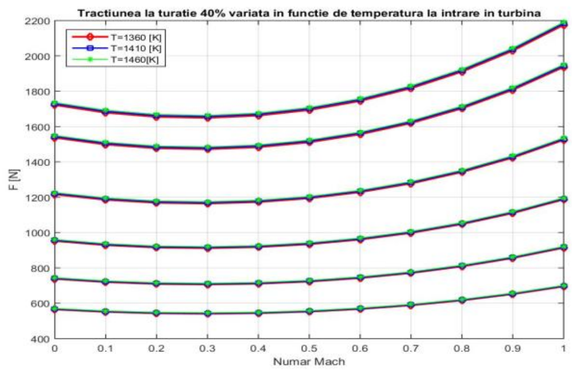

FIG. 12 - Comparison of Engine Thrust [N]. cruise speed = 0.9, T3T =1360, 1410, 1460 [K],

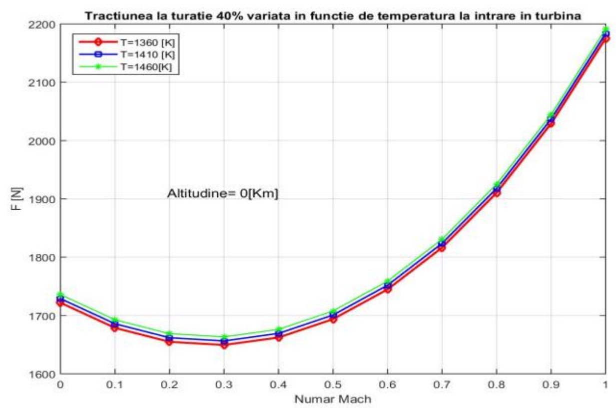

FIG. 13 - Comparison of Engine Thrust [N]. ground idling speed = 0.4, H = 0 [km],
T3T =1360, 1410, 1460 [K],

5. CONCLUSIONS & ACKNOWLEDGMENT

The investigation presented in this paper is focused on the influence of the variation of the turbine inlet temperature, as perturbation of the engine's design parameter and altitude Mach number and speed as perturbations of the flight and engine operating regimes.

The objective of this study is to highlight the variation of engine's thrust for a given perturbation of the turbine inlet temperature. The turbine inlet temperature ranges between 1360 and 1460 [K], which corresponds to a perturbation of +/- 50 [K] with respect to the reference value, that is considered at the engine's design point.

The predicted performances of the turbojet engine (i.e. thrust, specific thrust and fuel specific consumption) are summarized in Fig. 1 ÷ Fig. 9. In Fig. 10÷ Fig. 13 is summarized a comparison of the variation of thrust with the temperature T3T, for different rotor speed, flight Mach number and altitude. From Fig. 10÷ Fig. 13 comes out that the influence of T3T temperature perturbation on thrust is larger with the variation of rotor speed than with the flight velocity.

This observation can to direct the future developments of this study towards the establishing of a new command and control law for the turbofan engine operation. Further, the practical applications of this study can be related to be used both for training the pilot students and during flight operation, for contributing to an improvement in flight safety, which can be of real help for fighter pilots.

The authors would like to express their gratitude to the INCAS - National Institute of Aerospace Research "Elie Carafoli" Bucharest for the support while carrying on research activities within the Flow Physics Department, Numerical Simulations Unit, as well as the documentary research. The results presented in this paper are correlated to the current research activities regarding the jet propulsion systems, carried on within INCAS.

REFERENCES

[1] J. D. Mattingly, *Elements of Propulsion and Gas Turbine and Rockets,* American Institute of Aeronautics and Astronautics Education Series, Inc. Reston, VA,.2006

[2] ***, Rolls Royce, *The Jet Engine*, fifth edition, ISBN 0 902121 2 35, The Technical Publications Department Rolls-Royce plc, Derby, England

[3] ***, Powerplant, JAA ATPL Training, JEPPESEN, Atlantic Flight Training Ltd

[4] Wilfried Wisser, *Generic Analysis Methods for Gas Turbine Engine Performance, The development of the gas turbine simulation program GSP*, PhD Thesis, NLR and TU Delft, 2015.

[5] ***, *Compressor and Turbine Maps for Gas Turbine Performance Computer Programs*, Issue 3, GasTurb GmbH, 2013

[6] NASA Technical Memorandum **TM X-3014**, *A generalized hybrid computer program for studying turbojet or turbofan engine dynamics*, John Szuch, Cleveland, Ohio, 1974

[7] S. M. Eastbourn, *Modeling and simulation study of a dynamic turbofan engine using Matlab Simulink*, M. Sc. A.E. Dissertation, Wright State University, 2012

[8]. Pimsner V., *Motoare aeroreactoare*, Ed. Didactica si Pedagogica, Bucuresti, 1983

[9] Irina Andrei, Adrian Toader, Gabriela Stroe, Florin Frunzulica, *Performance Analysis and Dynamic Modeling of a Single-Spool Turbojet Engine*, International Conference in Nonlinear Problems in Aviation and Aerospace ICNPAA 2016, La Rochelle, France, AIP Conference Proceedings,

[10] Gabriela Stroe, Irina Andrei, Florin Frunzulica, *Analysis of Control System Responses for Aircraft Stability and Efficient Numerical Techniques,* International Conference in Nonlinear Problems in Aviation and Aerospace ICNPAA 2016, La Rochelle, France, AIP Conference Proceedings,

[11] Irina Andrei, Mihai Niculescu, Mihai Victor Pricop, Andreea Cernat, *Study of the Turbojet Engines as Propulsion Systems for the Unmanned Aerial Vehicles,* AFASES 2016, AFAHC Brasov, 2247-3173, Diseminare Proiect MASIM

[12] Alexandru Ionel, Stefan Palas, Irina Andrei, *Performance Analysis of the IAR 99 SOIM and IAR 99 TD,* AEROSPATIAL 2016, INCAS, ISSN 2067-8614

[13] Andreea Cernat, Alexandru Ionel, Irina Andrei, Stefan Palas, Adrian Mihai, *Simulation Tool for Predicting Ground Test Performances of a Turbofan Propulsion System Air Inlet,* AEROSPATIAL 2016, INCAS, ISSN 2067-8614

[14] Irina Andrei, Alexandru Ionel, Adrian Mihai, Stefan Palas, Tiberiu Salaoru, *Numerical Modeling Application for Simulating Engine Test Cell Validation Methodlogy of a Turbofan Exhaust System,* AEROSPATIAL 2016, INCAS, ISSN 2067-8614

[15] Irina Andrei, Alexandra Stanescu, Adrian Toader, *Issues on the completion of the mathematical model by Parameter Identification for Simulating a Jet Engine,* NMAS 2016, INCAS, ISSN 2360-1809

[16] Vasile Prisacariu, Ionica Circiu, *Considerations Regarding the Performances of the Combustion Chambers for Turbojet Engines,* Review of the Air Force Academy, No 2 (32) 2016 DOI: 10.19062/1842-9238.2016.14.2.7

[17] Irina Andrei, Adrian Toader, Ana Maria Neculaescu, *Numerical Simulations of Steady-State and Dynamic Analysis of a Single-Spool Turbojet Engine,* NMAS 2016, INCAS, ISSN 2360-1809

[18] Dr. I. Andrei, A. Stanescu, *Issues on modeling and simulation of a mixed flows turbofan*, Caius Iacob Conference, 2015

[19] Ciobotea V., *Teoria motoarelor de aviatie, vol. 1*, Editura Academie Militare, Bucuresti, 1978;

[20] Manole I., *Solutii constructive de turbomotoare de aviatie (album de scheme), vol. 1,* Editura Academiei Militare, Bucuresti, 1977;

[21] Rotaru C., Mihaila-Andres M., Pericle G.M., Edu R. I., *Thermodynamic performances of the turbojet combustion chambers – numerical evaluation*, Proceedings of the 2014 International Conference on Mechanics, Fluid Mechanics, Heat and Mass Transfer, p. 86-91, 2014;

[22] Rotaru C., Cîrciu I., Arama C., Constantinescu C., *Aspects regarding velocity distribution in the secondary zone o a gas turbine combustor,* Review of the Air Force Academy, 2/2015, DOI: 10.19062/1842-9238.2015.13.3.5, p. 33-38, 2015;

[23] Rotaru C., Andres-Mihaila M., Pericle G.M., *An Extended Combustion Model for the Aircraft Turbojet Engine*, International Journal of Turbo & Jet-Engines, 3/2014, p.229-237, 2014.

[24] Farokhi S., *Aircraft propulsion,* second edition, Wiley and sons, 2014;

[25] Stefanescu I., *Advanced Training Aircraft IAR 99 (A) SOIM*, INCAS BULLETIN, vol. 4, Issue 2/2012, DOI: 10.13111/2066-8201.2012.4.2.13,pp. 125 – 135, 2012;

[26] F. Zare, Dr. Arpad Veress, K. Beneda, *Simplified mathematical model for a single spool and no by-pass jet engine*, RTK Conference, BME, 2013

[27] H. Asgari, X. Chen, R. Sainudin, *Modeling and simulation of gas turbines*, Intl. Journal Modelling, Simulation and Control, 2013.

[28] S. C. Uysal, *High by-pass ratio turbofan engines aero-thermodynamic design and optimization*, PhD Thesis, The Graduate School of Natural and Applied Sciences, Middle East Technical University, 2014

[29] NASA Technical Memorandum 83446 (NASA - TM 83446), *Digital Computer Program for Generating Dynamic Turbofan Engine Models (DIGTEM)*, C.J. Daniele, S. M. Krosel, J. R. Szuch, E. J. Westerkamp, Lewis Research Center, Cleveland, Ohio, 1983